

IV–VI compound midinfrared high-reflectivity mirrors and vertical-cavity surface-emitting lasers grown by molecular-beam epitaxy

Z. Shi,^{a)} G. Xu, P. J. McCann, and X. M. Fang

School of Electrical and Computer Engineering, and Laboratory for Electronic Properties of Materials, University of Oklahoma, Norman, Oklahoma 73019

N. Dai

Department of Physics and Astronomy and Laboratory for Electronic Properties of Materials, University of Oklahoma, Norman, Oklahoma 73019

C. L. Felix, W. W. Bewley, I. Vurgaftman, and J. R. Meyer

Naval Research Laboratory, Washington, DC 20375

(Received 20 January 2000; accepted for publication 28 April 2000)

Midinfrared broadband high-reflectivity $\text{Pb}_{1-x}\text{Sr}_x\text{Se}/\text{BaF}_2$ distributed Bragg reflectors and vertical-cavity surface-emitting lasers (VCSELs) with PbSe as the active material were grown by molecular-beam epitaxy. Because of an extremely high index contrast, mirrors with only three quarter-wave layer pairs had reflectivities exceeding 99%. For pulsed optical pumping, a lead salt VCSEL emitting at the cavity wavelength of 4.5–4.6 μm operated nearly to room temperature (289 K). © 2000 American Institute of Physics. [S0003-6951(00)04425-9]

Due to a variety of important applications, recent years have seen a world-wide increase in mid-IR semiconductor laser research. Much of that interest derives from the prospects for ultrahigh-sensitivity chemical detection¹ using inexpensive and portable spectroscopy instruments. Performance requirements that are not yet available include continuous wave (cw) operation at room temperature (or at least the thermoelectric cooler range of $T \geq 240$ K), spectral purity, and reasonable output powers (≥ 1 mW) with good beam quality. Currently, IV–VI lead salts,^{2–4} quantum cascade (QC)^{5,6} and type-II quantum well (QW) diode lasers^{7–9} are the leading approaches being pursued to meet these application needs. All have demonstrated above room-temperature operation in pulsed mode. However, high-temperature continuous wave (cw) lasing has been reported only for optically pumped type-II QW devices (up to 290 K).⁸ The highest $\text{cw}T_{\text{max}}$ obtained with electrical pumping was 223 K for a lead salt laser.²

For a number of years lead salt diodes have been the only commercially available semiconductor mid-IR lasers. Their performance remains far from that desired, however, because of the low operating temperatures and low efficiencies (single-mode output powers are typically ≤ 1 mW even at 77 K). There is also a tendency toward multimode operation and mode hopping. Lasing thresholds are significantly increased by the fourfold degeneracy of the L-valley conduction and valence band extrema. Quantum confinement does not lift the degeneracy in edge-emitting QW devices, since the four valleys remain symmetric for the (100) growth that must be employed to allow for the cleaving of laser cavities. This prevents the full exploitation of what is perhaps the greatest advantage of IV–VI laser materials for high-temperature and long-wavelength operation, namely the threshold reduction that results from a low nonradiative recombination rate. Auger coefficients are typically an order of

magnitude smaller^{10,11} than those in type-II QWs, which are in turn significantly suppressed relative to other III–V and II–VI semiconductors with the same energy gaps.¹²

We point out in this letter that lead salt vertical-cavity surface-emitting lasers (VCSELs) may overcome many of the main limitations of IV–VI edge-emitters, and once optimized should provide an attractive high-temperature, single-mode, cw source for spectroscopy and other mid-IR applications. First, the short vertical cavity, when combined with a small lateral dimension on the order of one to three wavelengths, should produce a temporally stable single-mode output of high spectral purity. Second, since no cleaving is required the laser structures may be grown on (111) BaF_2 substrates, which for many years have been used routinely to fabricate high-quality nonlaser IV–VI structures.¹³ Besides taking advantage of a factor of 5 enhancement of the room-temperature thermal conductivity in BaF_2 over that in PbSe, this configuration will allow the growth of QW VCSELs in which the degeneracy of the L valleys is lifted. The reduction of the threshold carrier concentration by up to a factor of four should make room-temperature cw operation quite feasible. The efficiency may also be enhanced significantly, not only because free carrier absorption losses are reduced but also because the much shorter effective cavity length in a VCSEL will allow a larger fraction of the mid-IR light to be emitted before it is reabsorbed. The thermal properties may benefit further from our planned application of the diamond pressure bond heat sinking technique.⁸

The optical cavity in a VCSEL is created by surrounding the active region with two distributed Bragg reflectors (DBR) mirrors. Since in our case the desired center wavelength is beyond 4 μm and the thickness of each period in the quarter-wave stack scales with λ , constraints on the total epitaxial thickness limit the number of periods that are practical to grow by molecular-beam epitaxy (MBE). It is therefore critical to choose high- and low-index stacking materials that have as large a contrast ratio as possible. In addition,

^{a)}Electronic mail: shi@ou.edu

TABLE I. Some relevant material parameters at room temperature, where α is the thermal expansion coefficient and E_g is the energy gap.

Material	Lattice constant (\AA)	α (10^{-6} K^{-1})	Refractive indices (at $4.7 \mu\text{m}$)	Thermal conductivity (W/cm K)	E_g (eV)
PbSe	6.124	19.4	5.0	0.018	0.265
Pb _{0.97} Sr _{0.03} Se	6.125	NA	4.7	NA	0.413
Pb _{0.85} Sr _{0.15} Se	6.128	NA	3.7	NA	0.826
BaF ₂	6.20	19.8	1.46	0.1	10.4

both components of the mirror should be lattice and thermal-expansion-matched to the underlying substrate. In all of these regards Pb_{1-x}Sr_xSe, which has been used as the confinement layer in PbSe-based diode lasers,^{14,15} and BaF₂ form an excellent DBR pair. Table I shows that while the lattice constant and thermal expansion coefficient for PbSe nearly match those of BaF₂, the contrast in refractive indices is very large, where the refractive indices of Pb_{1-x}Sr_xSe were determined by the transmission measurement. Consequently, a three-pair quarter-wave BaF₂/Pb_{0.97}Sr_{0.03}Se mirror can provide more than 99% peak reflectivity, as is apparent from the experimental spectrum illustrated in Fig. 1. The high-reflectivity plateau is seen to be quite broad, which widens the temperature range over which the VCSEL can be tuned. Moreover, the continuous, broadband cavity resonance eliminates mode hopping, which can severely complicate the use of Fabry-Perot mid-IR lasers in spectroscopy applications. The maximum reflectivity is comparable and the bandwidth much broader than for a recently reported mid-IR Pb_{0.99}Eu_{0.01}Te/Pb_{0.94}Eu_{0.06}TeDBR, which had 32 periods but a much lower contrast of the refractive indices.¹⁶ In this work, Pb_{0.97}Sr_{0.03}Se and Pb_{0.85}Sr_{0.15}Se were used for the bottom and top mirrors, respectively. As is shown in Table I, high Sr composition increases the energy band gap and keeps the top mirror transparent at the optical pumping wavelength.

A full VCSEL structure was grown by MBE in an Intevac Modular Gen II system. Cells for Sr, PbSe, BaF₂, and a Se valve cracker were used as sources. The background pressure was approximately 5×10^{-10} Torr before growth and 1×10^{-8} Torr during growth. Freshly cleaved BaF₂(111) substrates were baked at 500 °C for 10 min prior to growth and kept at 360 °C during growth. The growth rates were 0.8 $\mu\text{m}/\text{h}$ for PbSe and 0.6 $\mu\text{m}/\text{h}$ for BaF₂, respectively. A 0.6 μm BaF₂ buffer layer was grown first, followed by the

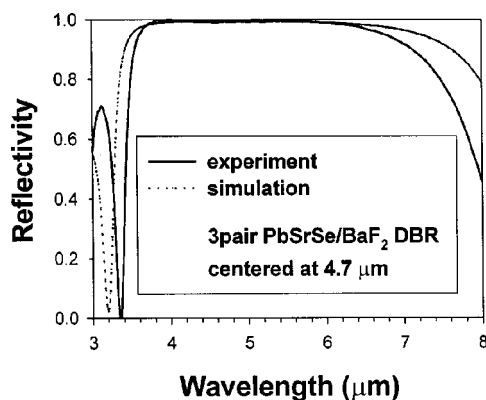
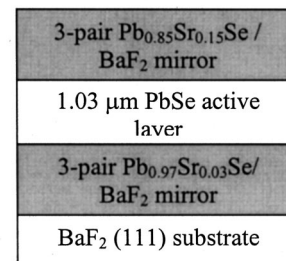


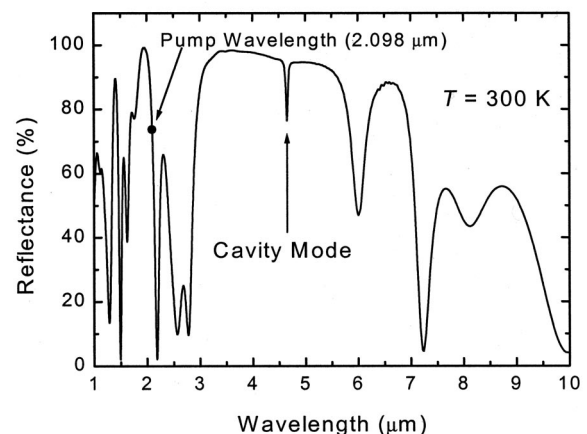
FIG. 1. Measured and simulated transmission spectra for a three-pair Pb_{0.97}Sr_{0.03}Se/BaF₂DBR.

VCSEL structure shown in Fig. 2(a). The λ cavity consisted simply of a 1.03 μm layer of PbSe. This cavity thickness was chosen so that the maximum overlap of the cavity mode with the gain peak would occur at an intermediate temperature.

The reflectivity spectrum for this structure is given in Fig. 2(b). The central plateau is seen to contain a distinct dip corresponding to the cavity mode. The design of the top DBR mirror was intended to place the pump wavelength of 2.098 μm in a low-ripple region of the reflectivity interference fringes. However, due to some 3% error in the growth thickness, the spectrum shifted such that at normal incidence the pump wavelength actually fell in a region with a relatively high reflectivity of $\approx 75\%$, as indicated in Fig. 2(b). Our model projects 50% reflectivity at that wavelength for the 37° pump angle that was employed in the experiments, so lowering of this reflectivity could increase the power conversion efficiencies and reduce the threshold pump intensities reported below. We also note that the energy gap of the Pb_{0.85}Sr_{0.15}Se in the top DBR is larger than the pump photon energy.



(a)



(b)

FIG. 2. Layering sequence (a) and reflectivity (b) of the VCSEL structure. The dip in the middle of the reflectivity plateau provides a clear signature for the wavelength of the cavity mode.

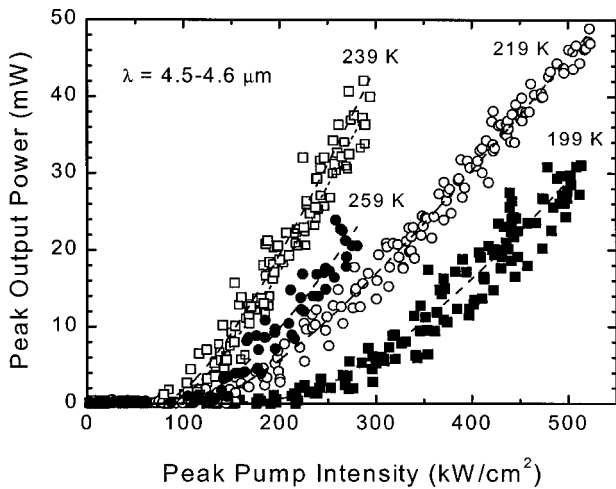


FIG. 3. Peak VCSEL output power vs peak pump intensity at four temperatures, for a $96\ \mu\text{m} \times 60\ \mu\text{m}$ pump spot.

With optical pumping by 100 ns Q -switched pulses from a Ho: yttrium-aluminum-garnet (YAG) laser ($2.098\ \mu\text{m}$) at an angle of 37° , the as-grown device displayed vertical-cavity lasing at temperatures between 199 and 289 K. For a pump-spot dimension of $96\ \mu\text{m} \times 60\ \mu\text{m}$ (multiple lateral modes), the spectral linewidth was relatively broad (≈ 50 nm). However, the shift of the peak wavelength with temperature was quite gradual, from $4.60\ \mu\text{m}$ at 209 K to $4.50\ \mu\text{m}$ at 279 K, since it followed the slow decrease of the refractive index, and hence the cavity resonance wavelength, with increasing T . The far-field pattern was nearly circular, with full width at half maximum divergence angles of 27° and 33° along the two axes perpendicular to the vertical emission. Figure 3 shows light-light curves at a series of temperatures. The maximum peak output powers of 49 mW at 219 K and 24 mW at 259 K have clearly not saturated.

Figure 4 plots dependences of both the threshold pump intensity and the optical power conversion efficiency on temperature. The minimum threshold was $69\ \text{kW}/\text{cm}^2$ at 239 K and the highest efficiency was $\approx 0.5\%$ at 239–249 K. Both properties are most favorable at intermediate rather than low

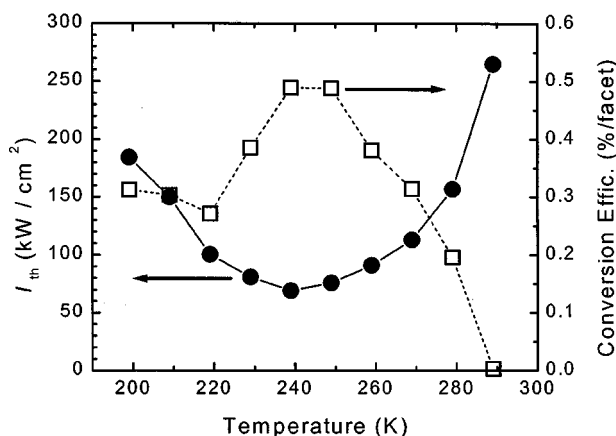


FIG. 4. Temperature-dependent threshold pump intensity and efficiency for the lead salt VCSEL.

temperatures because the overlap of the gain peak with the cavity wavelength is optimized for $T \approx 260$ K, and that overlap becomes poorer at both lower and higher T . Comparison with thresholds and efficiencies for the longest-wavelength III-V VCSEL¹⁷ ($\lambda = 2.9\text{--}3.0\ \mu\text{m}$) shows that the present lead salt results are slightly better at all $T > 240$ K, despite the longer wavelength ($\lambda = 4.5\text{--}4.6\ \mu\text{m}$). The maximum operating temperature and power conversion efficiencies are also much better than for a recent HgCdTe-based VCSEL which emitted at $2.6\ \mu\text{m}$.¹⁸

While the preliminary vertical-cavity lasing results reported here are quite encouraging, substantial improvements should be possible. Especially promising are the prospects for PbSe-based QW VCSELs, which are projected to have not only superior gain and differential gain properties due to the two-dimensional density of states, but also much lower thresholds and internal losses due to lifting of the valley degeneracy. At the same time, improvements in the device fabrication quality will be required before lead salt VCSELs can fully realize their potential. Ultimately, electrical injection and single-mode cw emission at thermoelectric cooler temperatures are envisioned.

Work at OU was partially supported by AFOSR. Work at NRL was supported in part by ONR while WWB held an ASEE/NRL Research Associateship.

¹M. Tacke, *Infrared Phys. Technol.* **36**, 447 (1995).

²G. Bauer, M. Kriechbaum, Z. Shi, and M. Tacke, *J. Nonlinear Opt. Phys. Mater.* **4**, 283 (1995).

³Z. Feit, M. McDonald, R. J. Woods, V. Archambault, and P. Mak, *Appl. Phys. Lett.* **68**, 738 (1996).

⁴U. P. Schliessl and J. Rohr, *Infrared Phys. Technol.* **40**, 325 (1999).

⁵J. Faist, F. Capasso, C. Sirtori, D. L. Sivco, J. N. Baillargeon, A. L. Hutchinson, S. G. Chu, and A. Y. Cho, *Appl. Phys. Lett.* **68**, 3680 (1996).

⁶S. Slivken, A. Matlis, A. Rybaltowski, Z. Xu, and M. Razeghi, *Appl. Phys. Lett.* **74**, 2758 (1999).

⁷H. Lee, L. J. Olafsen, R. J. Menna, W. W. Bewley, R. U. Martinelli, I. Vurgaftman, D. Z. Garbuzov, C. L. Felix, M. Maiorov, J. R. Meyer, J. C. Connolly, A. R. Sugg, and G. H. Olsen, *Electron. Lett.* **35**, 1743 (1999).

⁸W. W. Bewley, C. L. Felix, I. Vurgaftman, D. W. Stokes, E. H. Aifer, L. J. Olafsen, J. R. Meyer, M. J. Yang, B. V. Shanabrook, H. Lee, R. U. Martinelli, and A. R. Sugg, *Appl. Phys. Lett.* **74**, 1075 (1999).

⁹R. Q. Yang, J. D. Bruno, J. L. Bradshaw, J. T. Pham, and D. E. Wortman, *Electron. Lett.* **35**, 1254 (1999).

¹⁰R. Klann, T. Hofer, R. Buhleier, T. Elsaesser, and J. W. Tomm, *J. Appl. Phys.* **77**, 277 (1995).

¹¹P. C. Findlay, C. R. Pidgeon, B. N. Murdin, A. F. G. van der Meer, A. F. G. Langerak, C. M. Ciesla, J. Oswald, G. Springholz, and G. Bauer, *Phys. Rev. B* **58**, 12908 (1998).

¹²J. R. Meyer, C. L. Felix, W. W. Bewley, I. Vurgaftman, E. H. Aifer, L. J. Olafsen, J. R. Lindle, C. A. Hoffman, M.-J. Yang, B. R. Bennett, B. V. Shanabrook, H. Lee, C.-H. Lin, S. S. Pei, and R. H. Miles, *Appl. Phys. Lett.* **73**, 2857 (1998).

¹³G. Springholz, Z. Shi, and H. Zogg, *Thin Films: Heteroepitaxial: Systems*, edited by W. K. Liu and M. B. Santos (World Scientific, Singapore, 1999).

¹⁴Z. Shi, M. Tacke, A. Lambrecht, and H. Boettner, *Appl. Phys. Lett.* **66**, 2573 (1995).

¹⁵A. Lambrecht, N. Herres, B. Spanger, S. Kuhn, H. Boettner, M. Tacke, and J. Evers, *J. Cryst. Growth* **108**, 310 (1991).

¹⁶T. Schwarzl, G. Springholz, H. Seyringer, H. Krenn, S. Lanzerstorfer, and W. Heiss, *IEEE J. Quantum Electron.* **35**, 1753 (1999).

¹⁷C. L. Felix, W. W. Bewley, I. Vurgaftman, J. R. Meyer, L. Goldberg, D. H. Chow, and E. Selvig, *Appl. Phys. Lett.* **71**, 3483 (1997).

¹⁸C. Roux, E. Hadji, and J.-L. Pautrat, *Appl. Phys. Lett.* **75**, 3763 (1999).